

**Figure 2.** Reaction pathway for transmembrane redox. The  $k_2$  step, represented as viologen dimerization, is complex.

inside-outside  $MV^{2+}$  product distribution after redox cycling was very nearly identical with the initial distribution before reduction. This result is expected since transmembrane oxidation of internal  $MV^+$  would be electrogenic in the opposite sense to internal  $MV^{2+}$  reduction in the absence of transverse ion migration. Thus, the same forces driving inward diffusion of  $MV^+$  during reduction drive its outward diffusion when a membrane-impermeable oxidant is used.

Reduction of  $MV^{2+}$  bound only at the external interface of DHP vesicles gave predominantly monomeric radical ion product<sup>16</sup> (Figure 1, solid line). The amount of monomer remained greater than 85% of the total reduced viologen at  $[MV^{2+}]/[DHP]$  ratios ranging from 0.0025–0.015 and was still 40% at the very high ratio of 0.15. In contrast, when equimolar  $MV^{2+}$  was present at the opposing vesicle interfaces or when internal  $MV^{2+}$  was in excess ( $r = 0.01$ –0.04), the product optical spectrum corresponded primarily to the multimeric form of the radical<sup>16</sup> (Figure 1, dotted line). When external  $MV^{2+}$  was in excess, the amount of multimer formed was approximately equal to the initial concentration of  $MV^{2+}$  on the inner surface, the remainder being monomeric  $MV^+$  radical cation (e.g., Figure 1, dot-dashed line). These observations indicate that the multimeric form of the radical is formed in a stoichiometric ratio of one viologen each from the inner and outer vesicle interfaces and that reduction of inner bound  $MV^{2+}$  is associated with aggregation.<sup>17</sup>

Reduction of DHP vesicles containing internally and externally bound  $MV^{2+}$  exhibited biphasic kinetics. Relative amplitudes for the two steps measured at various wavelengths indicated that monomeric and multimeric  $MV^+$  were the principal products of the fast and slow reaction steps, respectively. These observations establish that aggregation is coincident with transmembrane redox under steady-state conditions. With  $S_2O_4^{2-}$  in excess, the fast step was first order and gave a rate constant,  $k_1$ , similar to the constant for dithionite reduction of  $MV^{2+}$  in solution.<sup>18</sup> The rate for the slow step was about  $10^2$ -fold less than the fast reaction step and with equimolar  $MV^{2+}$  initially at both interfaces followed simple second-order kinetics with  $k_2 = 1.3 (\pm 0.4) \times 10^4 \text{ M}^{-1} \text{ s}^{-1}$  in 20 mM Tris, pH 8.0, 23 °C,  $[DHP] = 1$ –2 mM, and  $[MV^{2+}]/[DHP]$

$= 0.025$ – $0.081$ ;  $k_2$  was independent of the monitoring wavelength and  $S_2O_4^{2-}$  concentrations measured over the range  $[S_2O_4^{2-}] = 0.41$ – $2.2$  mM.

A reaction scheme consistent with these facts is illustrated in Figure 2. Here, rapid reduction of externally bound  $MV^{2+}$  ( $k_1$ ) precedes reduction of internally localized  $MV^{2+}$  ( $k_2$ ), which occurs either by rate-limiting formation of a mixed-valent  $MV^{2+}$ – $MV^+$  dimer or slow electron exchange between external  $MV^+$  and internal  $MV^{2+}$ , followed by rapid dimerization. The  $MV^{2+}$ – $MV^+$  dimer is subsequently rapidly reduced ( $k_3$ ) to  $(MV^+)_2$  by externally localized  $S_2O_4^{2-}$ . Upon oxygenation, the  $MV^{2+}$  ions derived from the dimer are found inside the vesicle, as expected from the system electrostatics. Since  $k_1, k_3 \gg k_2$ , the rate law is given by  $d[MV^+]_T/dt = k_1[MV^{2+}]_o[SO_2^-] + k_2[MV^+]_o[MV^{2+}]_i$ , where subscripts T, o, and i refer to total  $MV^+$  in the system and  $MV^{2+}$  bound at outer and inner vesicle interfaces, respectively. With equimolar inner and outer  $[MV^{2+}]$ ,  $[MV^+]_o \approx [MV^{2+}]_i$  for the slow step, so that  $d[MV^+]_T/dt \approx k_1[MV^{2+}]_o[SO_2^-] + k_2[MV^{2+}]_o^2$ .

Our present efforts are directed at probing mechanistic details of the transmembrane redox step and exploring the generality of the mechanism. Consistent with our observations, a report has recently appeared<sup>9</sup> suggesting comparable dynamic behavior for  $N,N'$ -dihexadecyl-4,4'-bipyridinium<sup>2+</sup>-mediated transmembrane electron transfer between  $S_2O_4^{2-}$  and  $Fe(CN)_6^{3-}$  ions separated by phosphatidylcholine liposomal membranes.

**Acknowledgment.** J.K.H. gratefully acknowledges stimulating discussions with Stephen W. Feldberg, insightful comments from several reviewers, and financial support from the Office of Basic Energy Sciences, U.S. Department of Energy (DE-FG06-87ER13664).

**Registry No.** DHP, 2197-63-9;  $MV^{2+}$ , 4685-14-7;  $S_2$ , 14844-07-6.

### Moderately Strong Intramolecular Magnetic Exchange Interaction between the Copper(II) Ions Separated by 11.25 Å in $[L_2Cu_2(OH)_2(\mu\text{-terephthalato})](ClO_4)_2$ ( $L = 1,4,7$ -Trimethyl-1,4,7-triazacyclonane)

Phalguni Chaudhuri,<sup>\*,1a</sup> Karen Oder,<sup>1a</sup> Karl Wieghardt,<sup>1a</sup> Stefan Gehring,<sup>1b</sup> Wolfgang Haase,<sup>1b</sup> Bernhard Nuber,<sup>1c</sup> and Johannes Weiss<sup>1c</sup>

*Lehrstuhl für Anorganische Chemie I, Ruhr-Universität  
D.4630 Bochum, Federal Republic of Germany  
Institut für Physikalische Chemie  
Technische Hochschule Darmstadt, D-6100 Darmstadt  
Federal Republic of Germany  
Anorganisch-Chemisches Institut der Universität  
D-6900 Heidelberg, Federal Republic of Germany  
Received November 30, 1987*

Owing to its fundamental importance, the study of long-range magnetic interactions has been an active field of research in recent years.<sup>2</sup> The terephthalato dianion has been proved to be an appropriate bridging unit to design magnetic systems with a separation of 11–12 Å between the two magnetic centers.<sup>3–5</sup> In all of these studies the intramolecular magnetic interactions, to the disappointment of the research workers, were negligibly small.

(1) (a) Ruhr-Universität. (b) Technische Hochschule Darmstadt. (c) Universität Heidelberg.

(2) *Magneto-Structural Correlations in Exchange Coupled Systems*; Willett, R. D., Gatteschi, D., Kahn, O., Eds.; Reidel: Dordrecht, The Netherlands, 1985.

(3) (a) Tinti, F.; Verdaguer, M.; Kahn, O.; Savariault, J. M.; *Inorg. Chem.* **1987**, *26*, 2380–2384, and references therein. (b) Julve, M.; Verdaguer, M.; Faus, J.; Tinti, F.; Moratal, J.; Monge, A.; Gutierrez-Puebla, E.; *Inorg. Chem.* **1987**, *26*, 3520–3527, and references therein.

(4) (a) Verdaguer, M.; Gouteron, J.; Jeannin, S.; Jeannin, Y.; Kahn, O. *Inorg. Chem.* **1984**, *23*, 4291–4296. (b) Bakalbassis, E. G.; Tsipis, C. A.; Mrozinski, J. *Inorg. Chem.* **1985**, *24*, 4231–4233. (c) Bakalbassis, E. G.; Mrozinski, J.; Tsipis, C. A. *Inorg. Chem.* **1986**, *25*, 3684–3690.

(5) Francesconi, L. C.; Corbin, D. R.; Clauss, A. W.; Hendrickson, D. N.; Stucky, G. D. *Inorg. Chem.* **1981**, *20*, 2078–2083.

(16) Meisel, D.; Mulac, W. A.; Matheson, M. S. *J. Phys. Chem.* **1981**, *85*, 179–187.

(17) Although the basis for preferential dimerization of  $MV^+$  within the vesicle is presently unknown, it is not ascribable simply to a concentrating effect. The internal surface area of the DHP vesicles is about 1/3 the total area;<sup>14</sup> because the viologen is extensively membrane-associated, the inner localized  $MV^+$  would be only twice the surface concentration of outer localized  $MV^+$  when the inside/outside ratio is equimolar.

(18) Tsukahara, K.; Wilkins, R. G. *J. Am. Chem. Soc.* **1985**, *107*, 2632–2635.

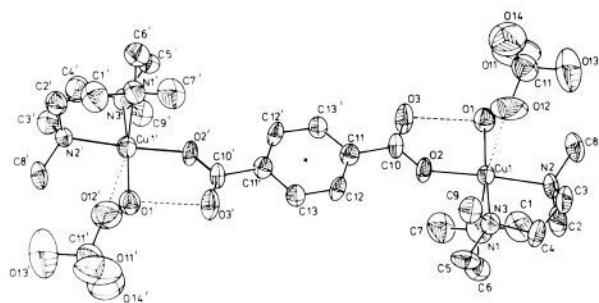


**Figure 1.** Structure of  $[L_2Cu_2(OH_2)_2(\mu\text{-terephthalato})]^{2+}$ , showing 40% probability ellipsoids. Representative distances (Å) are as follows: Cu1–N1, 2.217 (5); Cu1–N2, 2.034 (5); Cu1–O1, 2.009 (4); Cu1–O2, 1.972 (4); Cu1–O12, 2.992 (6); Cu1–Cu1', 11.252 (4); O3–O1, 2.516 (4).

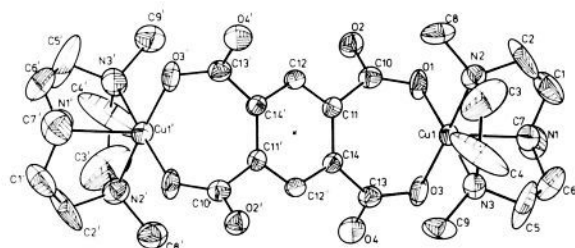


**Figure 2.** Structure of  $[L_2Cu_2(\mu\text{-tetracarboxylatobenzene})]$ , showing 40% probability ellipsoids. Representative distances (Å) are as follows: Cu1–N1, 2.188 (4); Cu1–N2, 2.035 (4); Cu1–O1, 1.942 (3); Cu1–O3, 1.949 (3); Cu1–Cu1', 7.811 (4).

We report here a long distance (11.3 Å) moderately strong antiferromagnetic coupling ( $J = -70 \text{ cm}^{-1}$ ) between Cu(II) atoms in a  $\mu$ -terephthalato complex. A second complex containing a  $\mu$ -tetracarboxylatobenzene bridging unit exhibits very weak exchange interactions although the Cu...Cu separation is smaller (7.8 Å) than that in the mentioned  $\mu$ -terephthalato complex. The X-ray structures of  $[LCu(OH_2)(\mu\text{-terephthalato})(OH_2)CuL](ClO_4)_2$  (**1**) and  $[LCu(\mu\text{-tetracarboxylato})CuL]\cdot 4H_2O$  (**2**) ( $L = 1,4,7$ -trimethyl-1,4,7-triazacyclononane)<sup>6</sup> are presented in Figures 1 and 2.

A crystallographic inversion center in **1** is located at the center of the benzene ring of the terephthalato ligand. The geometry around the two copper(II) ions is square-based pyramidal with two nitrogens N2 and N3 of the cyclic amine, one oxygen atom O2 of the carboxylic group, and the oxygen atom O1 of a water molecule in the basal plane and the nitrogen N1 of the amine in the apical position. The Cu(II) ion is displaced by 0.122 (2) Å from the mean basal plane toward the apex. Two perchlorate ions are in the vicinity of the Cu(II) centers (Cu1–O12 = 2.992 (2) Å). The two mean basal planes containing the  $CuN_2O_2$  units are strictly coplanar with the terephthalato ligand with its eight carbon

**Table I.** Magnetic and ESR Data for **1** and **2**

compd	$J/\text{cm}^{-1}$	$\langle g \rangle_{\text{mag}}$	$g_{\parallel}$	$g_{\perp}$
<b>1</b>	-70.0	2.20	2.30	2.10
<b>2</b>	-0.7	2.07	2.08	2.03

atoms. A strong hydrogen bond<sup>11</sup> (O3–O1 = 2.516 Å) may be envisaged between O1 of the coordinated water molecule and the noncoordinated oxygen atom O3 of the terephthalato anion, yielding a six-membered ring and enforcing the coplanarity of the planes of the terephthalato dianion with the mean basal plane containing the  $CuN_2O_2$  units. The Cu...Cu distance inside a dinuclear unit is 11.252 (4) Å. The closest intermolecular Cu...Cu distance is 7.587 (1) Å.

The dinuclear units in **2** are also centrosymmetric. The copper environments are very similar to that of **1**, i.e., square-based pyramidal. Each carboxylic group is bound to Cu(II) in a monodentate fashion through only one oxygen atom, yielding two seven-membered rings. The two basal planes containing the O1, O3, N2, and N3 atoms are parallel to each other but make the angles 116° and 64° with the Cu–Cu vector. A Cu...Cu separation of 7.811 (4) Å inside a dinuclear unit has been found.

Variable temperature (4.2–289.5 K) magnetic susceptibility<sup>6</sup> data of dried powdered samples of **1** and **2** were fitted by means of least squares to the expression<sup>7</sup> for  $\chi_M$  versus  $T$  derived from the isotropic spin Hamiltonian,  $\hat{H} = -2J\hat{S}_1\hat{S}_2$ , with  $S_1 = S_2 = 1/2$ . The results of susceptibility-fitting are listed in Table I. The X-band powder EPR spectra at 110 K of **1** and **2** are of axial type yielding two  $g$  values (Table I).<sup>8</sup>

The close-to-square-pyramidal geometry of the copper(II) ions in both compounds, **1** and **2**, suggests that they have  $(d_{x^2-y^2})^1$  ground states, as is also evident from the ESR spectra. The major  $\sigma$ -pathway<sup>10</sup> in **1** for the interaction of these magnetic orbitals containing the unpaired electron involves the terephthalato ligand, which is coplanar with the  $d_{x^2-y^2}$  orbital. Substantial antiferromagnetic coupling ( $J = -70 \text{ cm}^{-1}$ ) is therefore observed in **1**, in spite of the Cu...Cu intramolecular separation of 11.252 (4) Å. On the other hand, the noncoplanarity of the bridging ligand 1,2,4,5-tetracarboxylatobenzene with the plane of the magnetic orbitals of Cu(II),  $(d_{x^2-y^2})^1$ , leads to the weak magnetic interaction ( $J = -0.7 \text{ cm}^{-1}$ ) in **2**.

In summary, this work has shown that 11.25 Å is definitely not the limit for the intramolecular magnetic interaction between two Cu(II) ions, provided the Cu(II) atoms and the bridging ligand have the proper geometry.<sup>12</sup> A relatively strong magnetic interaction propagated through the bridging ligand along such a distance (11.25 Å) between two copper ions has been observed.

**Acknowledgment.** We thank the Fonds der Chemischen Industrie for financial support of this work.

**Supplementary Material Available:** A drawing of the unit cell of **1**, tables of positional and thermal parameters and bond distances and angles for **1** and for **2**, and two figures showing the fitted susceptibility curves (14 pages). Ordering information is given on any current masthead page.

(6) (a) Piperidinium terephthalate (0.5 mmol) was reacted with  $Cu(ClO_4)_2 \cdot 6H_2O$  (1 mmol) and 1,4,7-trimethyl-1,4,7-triazacyclononane(L)<sup>13</sup> (1.5 mmol) in methanol (50 mL) and upon concentration yielded turquoise blue crystals of compound **1**. Compound **2** was prepared similarly by reacting an aqueous solution (pH 9) of 1,2,4,5-tetracarboxylatobenzene (0.5 mmol) with a methanolic solution of  $Cu(AC)_2 \cdot H_2O$  (1 mmol) (40 mL) and L (1.5 mmol). (b) Analytical, magnetic, and spectroscopic data. Anal. Calcd for  $Cu_2C_{26}H_{46}N_6Cl_2O_{14}$  (**1**): C, 36.12; H, 5.36; N, 9.72; Cu, 14.70;  $ClO_4$ , 23.02. Found: C, 36.0; H, 5.60; N, 9.62; Cu, 14.86;  $ClO_4$ , 23.20. Anal. Calcd for  $Cu_2C_{28}H_{52}N_6O_{12}$  (**2**): C, 42.47; H, 6.62; N, 10.61; Cu, 16.05. Found: C, 42.31; H, 6.81; N, 10.30; Cu, 15.91. IR (KBr  $cm^{-1}$ ) 3560, 3480 (OH), 1570 and 1360 (COO), 1090, 610 ( $ClO_4$ ) for **1**, 3400 (br, OH), 1590 and 1370 (COO) for **2**. Magnetic measurements were repeated three times. For magnetic measurements crystals of **2** were powdered and dried under vacuum at 60 °C over  $P_2O_5$  for 90 h. Magnetic susceptibility [(T, K)  $\mu_B/Cu$  atom]: (4.2) 0.290, (25.8) 0.389, (55.9) 0.708, (103.4) 1.243, (149.2) 1.498, and (289.5) 1.792 for **1** and (4.2) 1.548, (25.8) 1.680, (55.9) 1.737, (149.2) 1.736, and (289.5) 1.796 for **2**. (c) **1** is monoclinic, space group  $P2_1/c$  ( $C_{2h}^2$ , no. 14) with  $a = 8.619$  (4) Å,  $b = 14.059$  (3) Å,  $c = 15.156$  (9) Å,  $\beta = 96.25$  (4)°,  $Z = 4$ ,  $R = 4.8\%$  for 1836 unique reflections ( $I \geq 2.5\sigma(I)$ ). **2** is orthorhombic, space group  $Pbca$  ( $D_{2h}^{15}$ , no. 61) with  $a = 14.400$  (4) Å,  $b = 16.963$  (5) Å,  $c = 16.879$  (7) Å,  $Z = 4$  and  $R = 5.4\%$  for 3558 observed ( $I \geq 2.5\sigma(I)$ ) reflections.

(7) O'Connor, C. J. *Prog. Inorg. Chem.* **1982**, *29*, 203–283, and references therein.

(8) The zero-field splitting (D)<sup>9</sup> could be calculated to be  $1.8 \times 10^{-3} \text{ cm}^{-1}$  for **1** and  $4.9 \times 10^{-3} \text{ cm}^{-1}$  for **2** by assuming that it arises from the dipolar interaction between the two local doublets separated by 11.25 and 7.81 Å, respectively.

(9) Abragam, A.; Bleaney, R. *Electron Paramagnetic Resonance of Transition Ions*; Clarendon: Oxford, England.

(10) (a) The crystal packing diagram (Supplementary Material), devoid of any preferential packing direction, clearly rules out the possibility of intermolecular magnetic interactions. (b) The  $PF_6^-$ -salt of the cation in complex **1** also exhibits an antiferromagnetic interaction with an S–T gap of 50  $cm^{-1}$ .

(11) The compound  $[Cu_2(bipy)_2(OH_2)(\mu\text{-terephthalato})]^{2+}$  of ref 4b also exhibits a moderately strong antiferromagnetic interaction ( $J = -25.9 \text{ cm}^{-1}$ ). Lacking crystal structure determination, this interaction has been interpreted as intermolecular in nature. It seems very likely that this compound also contains this type of hydrogen bonds and the magnetic interaction is intramolecular in nature.

(12) Kahn, O. *Angew. Chem.* **1985**, *97*, 837–853 *Angew. Chem., Int. Ed. Engl.* **1985**, *24*, 834.

(13) Chaudhuri, P.; Wieghardt, K. *Prog. Inorg. Chem.* **1987**, *35*, 329–436.